Expression and function of lncRNA ANRIL in a mouse model of acute myocardial infarction combined with type 2 diabetes mellitus

Lin Zhang[a,*,1], Yan-Min Wang[b,1]

[a]Department of Cardiology, Daqing Oilfield General Hospital, Daqing, Heilongjiang, China; [b]Department of Circulatory Medicine, Daqing Longnan Hospital, Daqing, Heilongjiang, China

Abstract

Background: This study intends to explore whether lncRNA ANRIL has an influence on type 2 diabetes mellitus (T2DM) complicated with acute myocardial infarction (MI) and to further investigate the underlying mechanism.

Methods: The ANRIL level in peripheral blood from patients was detected by qRT-PCR. A T2DM mouse model was established by intraperitoneal injection of streptozocin (STZ). MI was induced by ligation of the left anterior descending coronary artery. Cardiac function parameters were measured using echocardiography. Triphenyltetrazolium chloride (TTC) staining was performed to determine the infarct size, and Masson staining was conducted to delineate the area of fibrosis in the myocardium. TUNEL staining was used to detect myocardial cell apoptosis. The expression of the myocardial fibrosis-related proteins TGF-β1, collagen I and collagen III was analysed using Western blot.

Results: ANRIL was upregulated in peripheral venous blood from patients with T2DM-MI and in myocardial tissues from the established T2DM-MI model mice. Furthermore, ANRIL overexpression caused cardiac dysfunction and increased the heart/body weight rate and infarct size in the T2DM-MI mice. Moreover, ANRIL overexpression caused myocardial fibrosis and myocardial cell apoptosis, and it increased the expression of the myocardial fibrosis-related proteins TGF-β1, collagen I and collagen III in the T2DM-MI mice. However, ANRIL knockdown exerted the opposite effects.

Conclusion: ANRIL may be involved in the progression and development of T2DM-MI, which might provide novel ideas for the prevention and treatment of cardiovascular diseases.

Keywords: Acute myocardial infarction; lncRNA ANRIL; Type 2 diabetes mellitus

1. INTRODUCTION

Diabetes mellitus (DM) is an independent risk factor for acute myocardial infarction (MI) in European and Asian individuals.[1] DM patients were reported to have a larger infarct size, atypical ischaemic symptoms, and more post-infarct complications than non-diabetic patients.[2] It is well established that the clinical outcomes of acute MI in patients with type 2 diabetes mellitus (T2DM) are worse than those in non-diabetic patients.[3] It is reported that mortality, morbidity and re-infarction rates are higher following MI in diabetic than in non-diabetic individuals.[1] To date, the increased risk has been primarily attributed to hyperglycaemia, dyslipidaemia, a prothrombotic state in the pathogenesis of T2DM and its complications.[4] Further elucidation of the molecular mechanism underlying T2DM complicated with MI is of great importance for clinical treatment.

Long non-coding RNAs (lncRNAs) are mRNA-like transcripts longer than 200 bp that have no protein-coding potential.[5] LncRNAs play important regulatory roles in cancer cell growth, cell differentiation, cell metastasis and cell fate decision.[6,7] Antisense non-coding RNA in the INK4 locus (ANRIL), a 3.8 kb lncRNA located at the 9p21.3 locus within a gene cluster named INK4B-ARF-INK4A in the antisense direction, plays a role in the tumourigenesis of gliomas, breast cancer, and several other cancers.[8–11] The chromosome (Chr) 9p21 risk locus is associated with the severity, extent, and progression of coronary artery disease, indicating a role for this locus in influencing atherosclerosis and its progression.[12] ANRIL is essential in mediating Chr9p21 associations and has been reported to play an important role in many diseases, including Alzheimer disease, glaucoma, endometriosis, periodontitis, and particularly, T2DM.[13] In addition, ANRIL expression is associated with a risk for atherosclerosis at Chr9p21.[14] ANRIL may be implicated in the atherosclerotic process such as in thrombogenesis, vascular remodelling and/or repair, and plaque stability.[15] Furthermore, ANRIL is expressed in smooth muscle cells, endothelial cells and inflammatory cells known to be stimulated by atherosclerosis.[14–16] In addition, variants in ANRIL exons were found to contribute to MI risk in a Chinese Han population.[15] However, the expression and function of ANRIL in patients with T2DM complicated with acute MI (T2DM-MI) remain not fully elucidated.

*Address correspondence. Dr Lin Zhang, Department of Cardiology, Daqing Oilfield General Hospital, 9, Zhongkang Street, Daqing, Heilongjiang Province, 163001, China. E-mail address: zling0853@163.com (L. Zhang).

[1]Co-first authors.

Conflicts of interest: The authors declare that they have no conflicts of interest related to the subject matter or materials discussed in this article.

Journal of Chinese Medical Association. (2019) 82: 685-692.

Received March 2, 2018; accepted May 3, 2018.

10.1097/JCMA.0000000000000182.

<zdoi:10.1016/j.jcma.2018.05.004>

Therefore, this study aimed to investigate whether ANRIL expression has an influence on patients with T2DM-MI and to further explore the underlying mechanism. Here, we first detected the level of ANRIL in peripheral venous blood from T2DM-MI patients. A T2DM-MI mouse model was then constructed, and the effects of ANRIL on cardiac function, pathological changes, myocardial fibrosis, and myocardial cell apoptosis in the T2DM-MI mice were evaluated.

2. METHODS

2.1. Patients

Patients were recruited from the Daqing Oilfield General Hospital, including healthy controls (control group, n = 26), patients suffering from T2DM but not acute MI (T2DM group, n = 24), patients suffering from acute MI but not T2DM (MI group, n = 25), and patients suffering from acute MI and T2DM (T2DM-MI group, n = 34). The diagnosis of MI was made according to contemporary guidelines,[17] and the inclusion criteria for this study were described in a previous study.[18] The exclusion criteria were as follows: 1) impaired glucose tolerance, 2) diabetes due to secondary causes, and 3) past history of ischaemic heart disease. This research was approved by the local research ethics committee and was conducted in accordance with the Declaration of Helsinki. Written informed consent was obtained before any research procedures.

2.2. Animals

C57BL/6 male mice (aged 6–7 weeks, weighing 20 ± 2 g) were purchased from the animal laboratory of the Academy of Medical Sciences, Beijing, China. All mice used in this experiment were approved by the Ethic Committee of the Daqing Oilfield General Hospital. They were kept in separate cages and had free access to food and water in a room with 12 h light–dark cycles maintained at a temperature of 25 ± 1 °C and humidity of 50%.

2.3. Induction of T2DM mice

After being fasted overnight, mice (aged 6–7 weeks) received a single intraperitoneal (IP) injection of streptozocin (STZ, 50 mg/kg; Sigma–Aldrich, St Louis, MO, USA) for 5 days as previously described.[19] STZ is widely used in the induction of T2DM mouse models.[20] STZ solution was prepared fresh by dissolving it in 0.1 M citrate buffer (pH 5.5) and was terminally sterile-filtered. The normal group was injected with an equal amount of citrate buffer. After STZ injection, the fasting blood glucose of each mouse was measured for 3 days. Mice with fasting blood glucose levels higher than 11.1 mmol/L were considered T2DM mice and were used in the following experiment.

2.4. Establishment of the MI mouse model

T2DM mice were anaesthetized with ketamine (100 mg/kg; IP) and xylazine (5 mg/kg; IP) and were ventilated with a 1.0 inspired fraction of oxygen (FiO_2). MI was induced by ligation of the left anterior descending coronary artery (LAD) as previously described.[21] In brief, the LAD was exposed through a left thoracotomy, and a 7-0 silk suture was placed around the artery. Adequate LAD ligation was confirmed by a pale colour of the left ventricle (LV), S-T elevation and broadening of the QRS complex. After 30 min of ischaemia, the suture was loosened, and the polyethylene tube was removed. Reperfusion was confirmed, and the chest was then closed in layers. Finally, the mice were allowed to recover from anaesthesia.

2.5. Groups

Mice were divided into 5 groups (n = 10 in each group): the control group (control mice that were injected with an equal amount of citrate buffer for the T2DM control and then received sham surgery for MI), T2DM-MI group (T2DM and MI mice), T2DM-MI + vector group (T2DM and MI mice that were injected with 800 ng/kg empty plasmid into the infarcted area of the left ventricular wall), T2DM-MI + pcDNA-ANRIL group (T2DM and MI mice that were injected with 800 ng/kg ANRIL overexpression plasmid into the infarcted area of the left ventricular wall), and T2DM-MI + shRNA-ANRIL group (T2DM and MI mice that were injected with 800 ng/kg ANRIL knockout plasmid into the infarcted area of the left ventricular wall). The pcDNA3.1-lncRNA ANRIL (high expression plasmid) and pcDNA3.1-shLncRNA ANRIL (low expression plasmid) were made by Shanghai Genechem Co., Ltd. (Shanghai, China). The heart weight (mg)/body weight (g) ratio was calculated for all mice in each group as described previously.[22]

2.6. Echocardiography

At week 4 after the surgery, a non-invasive transthoracic echocardiography method was used to evaluate the structure and function of the left ventricle of each mouse as previously described.[23] In brief, mice were anaesthetized, and the parameters of heart structure and function were assessed in the two-dimensional ultrasound-guided M-curve. The parameters, including the left ventricular end-diastolic inner diameter (LViDd), left ventricular end-systolic inner diameter (LViD), left ventricular end-systolic volume (LVESV), left ventricular end-diastolic volume (LVEDV), ejection fraction (EF), fractional shortening (FS) and left ventricular mass (LVM), were automatically recorded. A Sino-Japanese joint AloCa5000 colour ultrasound diagnostic apparatus was used. Echocardiography was performed by a technician who was blinded to the experiment.

2.7. Triphenyltetrazolium chloride (TTC) staining

TTC was used for infarct size determination. Mice were anaesthetized, and then, the heart tissues were taken out and immediately frozen for 5 min at –20 °C. The hearts were sectioned from the apex to the base into five slices. One piece of tissue was sliced into 3 mm-thick sections, and these slices were put into 2% TTC solution and incubated at 37 °C for 20 min. The stained slices were immersed in 4% paraformaldehyde and fixed for 10 h. The non-infarcted myocardium was stained red, while the infarcted myocardium appeared white. The slices were photographed and analysed using Image-Pro Plus software (Media Cybernetics Inc, Silver Spring, MD, USA). Infarct size was expressed as a percentage of the mass of the whole myocardium.

2.8. Haematoxylin-eosin (HE) staining

The paraffin-embedded tissues were sliced into serial sections, after which they were stained with HE by using a routine staining procedure. The pathologic changes in these tissues were observed under light microscopy after HE staining. The slices were photographed and analysed using computerized Image-Pro Plus software.

2.9. Masson staining

Masson staining was performed to delineate the area of fibrosis in the myocardium. The paraffin-embedded tissues were sliced into serial sections and stained with Masson's trichrome. The fibrotic area was stained blue, while the viable area was stained red. Photographs were obtained, and the slides were observed under a stereomicroscope with the whole field view (8×).

2.10. TUNEL staining

Heart tissues were harvested and embedded with paraffin. The 4-μm-thick tissues were subjected to TUNEL staining according to the manufacturer's instructions for an *In Situ* Cell

Death Detection Kit (Cat. 11684817910, Roche Diagnostics, Indianapolis, IN, USA).

2.11. Western blot analysis

Protein was collected from myocardial tissues that were lysed in radioimmunoprecipitation assay buffer (RIPA) containing protease inhibitors for at 4 °C for 30 min. Cell lysates were prepared with a RIPA lysis buffer kit (Santa Cruz Biotechnology, Inc., Dallas, TX, USA). Subsequently, proteins were separated on 8% SDS-PAGE gels and transferred to polyvinylidene difluoride membranes (Amersham; GE Healthcare, Chicago, IL, USA). After blocking in 5% fat-free milk (Merck, Darmstadt, Germany) overnight at 4 °C, the transferred membranes were incubated with the following primary antibodies: TGF-β1 (1:160), collagen I (1:500), collagen III (1:100) and GAPDH (1:1000) overnight at 4 °C. After washing with TBST three times, the membranes were then incubated with a horseradish peroxidase-conjugated secondary antibody (1:1000, Goldenbridge Biotechnology Co., Ltd., Beijing, China; cat. A50-106P) at room temperature for 1 h. The protein was analysed using an enhanced chemiluminescence kit (ECL; Wuhan Booute Biotechnology Co., Ltd., China; Cat. orb90504). The band intensity was quantified with Quantity One software. GAPDH served as the loading control.

2.12. Reverse transcription-quantitative polymerase chain reaction (RT-qPCR)

Total RNA was isolated from peripheral blood or the myocardial tissues using TRIzol (Invitrogen) according to the manufacturer's protocol. Then, the isolated RNA was reverse transcribed into cDNA using a High Capacity cDNA Reverse Transcription Kit (Applied Biosystems; Thermo Fisher Scientific, Inc.). RT-qPCR was carried out using a SYBR® Premix Ex Taq™ Kit (TaKaRa Bio, Inc., Otsu, Japan) according to the manufacturer's instructions. The primer pairs used were as follows: lncRNA ANRIL, forward, 5′-TTATGCTTTGCAGCACACTGG-3′, and reverse, 5′-GTTCTGCCACAGCTTTGATCT-3′, and GAPDH, forward, 5′-ACCACAGTCCATGCCATCAC-3′, and reverse, 5′-TCCA CCACCCTGTTGCTGTA-3'. The relative expression of ANRIL was normalized to the internal control GAPDH. The comparative $2^{-\Delta\Delta Cq}$ method[24] was used to quantify gene expression levels.

2.13. Statistical analysis

All statistical analyses were performed using SPSS version 19.0 software (SPSS Inc., Chicago, Illinois, USA). Data are presented as the means ± standard deviation (SD) (x ± s). Statistical differences between two independent groups were determined using Student's t test. For multiple groups, the statistical analyses were performed by one-way analysis of variance (ANOVA). $p < 0.05$ was considered to indicate a statistically significant difference.

3. RESULTS

3.1. LncRNA ANRIL was upregulated in patients with T2DM-MI

As shown in Fig. 1, the serum expression of ANRIL from peripheral venous blood was significantly increased in T2DM patients compared with that in the controls ($p < 0.05$). The ANRIL expression in peripheral venous blood was also significantly increased in MI patients compared with that in the controls ($p < 0.05$). Importantly, the expression of ANRIL was significantly increased in peripheral venous blood from T2DM-MI patients compared with that from T2DM patients ($p < 0.05$) or MI patients ($p < 0.001$). These results indicated that increased expression of ANRIL is associated with the progression and development of T2DM complicated with MI.

3.2. Successful establishment of the T2DM-MI mouse model

C57BL/6 mice were fed a high-fat diet and injected intraperitoneally with STZ for 5 consecutive days to establish a model of T2DM. The normal control group was injected with an equal amount of citrate buffer. After STZ injection, the fasting blood glucose of each mouse was measured for 3 days. Mice with blood glucose higher than 11.1 mmol/L were confirmed as T2DM mice (Table 1). Furthermore, we measured insulin resistance-related parameters before MI surgery and confirmed that the T2DM mice were insulin resistant (Supplementary Table). After the establishment of the T2DM model, the MI model was established. Then, the cardiac function parameters in each group were measured using echocardiography. As shown in Table 2, LViDd, LViD, LVESV, LVEDV and LVM were significantly higher, but EF and FS were markedly lower in the T2DM-MI mice than in the control group ($p < 0.05$). Collectively, these results indicated that the T2DM-MI mouse model was successfully established.

3.3. Effects of lncRNA ANRIL on cardiac function and pathological changes in the T2DM-MI mice

The expression of ANRIL in myocardial tissues of the T2DM-MI mice was significantly upregulated compared with that of the control group (Fig. 2, $p < 0.001$). ANRIL was then overexpressed or knocked down in the mice (Fig. 2), and this

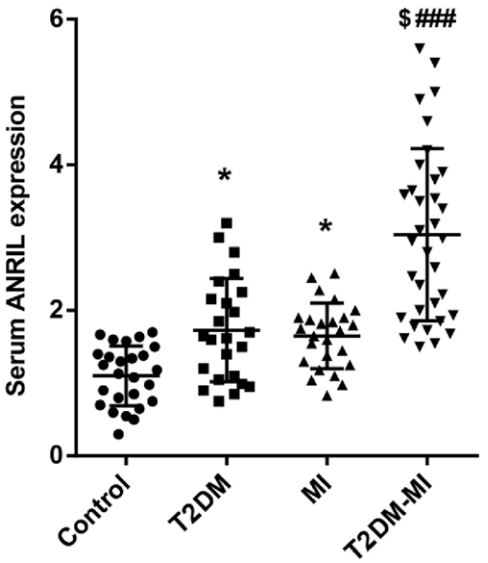

Fig. 1 LncRNA ANRIL was upregulated in patients with T2DM-MI. The expression of lncRNA ANRIL was significantly increased in peripheral venous blood from patients with T2DM-MI compared with that in MI patients ($p < 0.001$). n = 26 in the control group, n = 24 in the T2DM group, n = 25 in the MI group and n = 34 in the T2DM-MI group. *$p < 0.05$ *vs.* control group, $^{\$}p < 0.05$ *vs.* T2DM group and $^{\#\#\#}p < 0.001$ *vs.* MI group.

Table 1

Fasting blood glucose (FBG) of each group (n = 10 in each group, mmol/L).

Groups	Before STZ treatment	After STZ treatment
Control	6.75 ± 0.86	6.51 ± 0.90
T2DM	6.53 ± 0.92	13.67 ± 1.05[ab]

[a]$p < 0.05$, the T2DM+after STZ treatment group versus the Control+after STZ treatment group; [b]$p < 0.05$, the T2DM+after STZ treatment group versus the T2DM+before STZ treatment group. The normal control group was injected with an equal amount of citrate buffer. C57BL/6 mice were fed with high fat diet and injected intraperitoneally with streptozocin (STZ) for 5 days consecutively to establish model of T2DM.

Table 2

Cardiac function parameters of each group measured by echocardiography (n = 10 in each group).

Groups	LViDd (mm)	LViD (mm)	LVESV(μL)	LVEDV (μL)	EF (%)	FS (%)	LVM (mg)
Control	3.055 ± 0.1423	2.311 ± 0.1137	16.78 ± 2.813	46.12 ± 4.317	60.13 ± 2.304	66.83 ± 2.014	43.43 ± 2.677
T2DM-MI	4.625 ± 0.1303[a]	4.208 ± 0.1849[a]	83.45 ± 3.859[a]	94.65 ± 4.859[a]	23.45 ± 7.852[a]	46.48 ± 4.352[a]	68.23 ± 9.730[a]
T2DM-MI + vector	4.545 ± 0.1394[a]	4.201 ± 0.2147[a]	83.21 ± 4.121[a]	95.12 ± 5.479[a]	22.89 ± 8.869[a]	45.81 ± 4.012[a]	67.93 ± 7.815[a]
T2DM-MI + pcDNA-ANRIL	6.876 ± 0.1150[ab]	5.958 ± 0.2945[ab]	189.35 ± 4.106[ab]	149.32 ± 9.669[ab]	10.39 ± 5.736[ab]	29.63 ± 3.410[ab]	89.33 ± 6.802[ab]
T2DM-MI + shRNA-ANRIL	3.422 ± 0.1022[b]	2.632 ± 0.3852[b]	45.21 ± 4.325[ab]	61.29 ± 8.926[ab]	43.01 ± 2.035[ab]	58.28 ± 3.612[b]	51.19 ± 5.617[b]

[a]$p < 0.05$, versus the Control group; [b]$p < 0.05$, versus the T2DM-MI + vector group.

Followed by the establishment of T2DM models, the MI model was established, and the cardiac function parameters in each group were measured by echocardiography. The control mice were injected with an equal amount of citrate buffer for T2DM control and then received sham surgery for MI.

LViDd = the left ventricular end-diastolic inner diameter; LViD = left ventricular end-systolic inner diameter; LVESV = left ventricular end-systolic volume; LVEDV = left ventricular end-diastolic volume; EF = ejection fraction; FS = fractional shortening; LVM = left ventricular mass.

change in expression was confirmed by qRT-PCR. Furthermore, the effects of ANRIL expression on cardiac function and pathological changes were determined. As shown in Table 2, ANRIL overexpression significantly increased LViDd, LViD, LVESV, LVEDV and LVM but decreased EF and FS in the T2DM-MI mice ($p < 0.05$). In contrast, ANRIL knockdown significantly decreased LViDd, LViD, LVESV, LVEDV and LVM but increased EF and FS in the T2DM-MI mice ($p < 0.05$). These results indicated that ANRIL overexpression caused cardiac dysfunction in the T2DM-MI mice.

Comparison of pathological changes in each group was then conducted (Fig. 3A). According to observations under light microscopy, we found that the heart/body weight rate in the T2DM-MI mice was significantly increased compared with that in the control group ($p < 0.05$). Furthermore, ANRIL overexpression significantly increased the heart/body weight ratio in the T2DM-MI mice ($p < 0.05$). In contrast, ANRIL knockdown significantly decreased the heart/body weight rate in the T2DM + MI mice ($p < 0.05$) (Fig. 3B). We also found that the infarct size in the T2DM + MI mice was significantly increased compared with that in the control group ($p < 0.001$). Moreover, ANRIL overexpression significantly increased the infarct size compared with that in the T2DM-MI + vector group ($p < 0.01$). By contrast, ANRIL knockdown significantly decreased the infarct size in the T2DM mice ($p < 0.01$) (Fig. 3C).

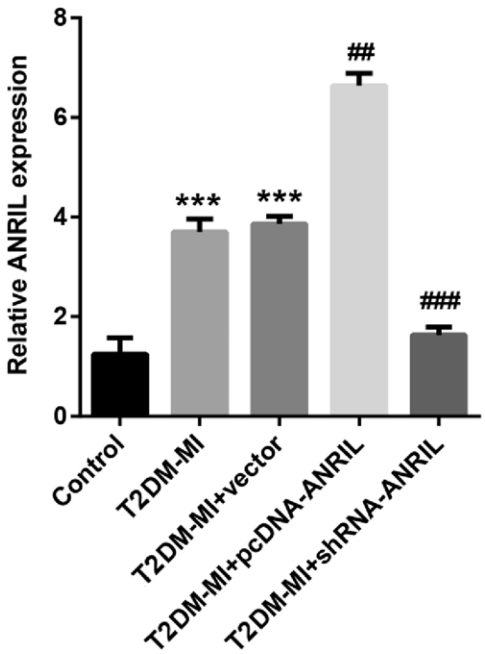

Fig. 2 The expression of lncRNA ANRIL in each group. The expression of ANRIL relative to GAPDH in myocardial tissues of the T2DM-MI mice was significantly upregulated compared with that in the control group. ANRIL was successfully overexpressed or knocked down in mice, and this change in expression was determined by qRT-PCR. n = 10 in each group. ***$p < 0.001$ *vs.* control group, ##$p < 0.01$, ###$p < 0.001$ *vs.* T2DM + vector group.

3.4. Effects of lncRNA ANRIL on myocardial pathology and fibrosis in the T2DM-MI mice

HE staining was performed to determine myocardial pathology (Fig. 4A), and Masson's trichrome staining was conducted to delineate the area of fibrosis in the myocardium (Fig. 4B). The data revealed that the myocardial tissue structure was complete and that no myocardial fibrosis was found in the control group. In the T2DM-MI and T2DM-MI + vector groups, we found that myocardial cells were stained unevenly, myocardial fibres were in a disordered arrangement, the gap was narrowed, and inflammation in the necrotic area was evident. In the T2DM-MI + pcDNA-ANRIL group, myocardial fibres were also in a disordered arrangement, a large number of fibroblasts were observed in the myocardial vasculature and mesenchyme, and hyperplasia of the fibrous connective tissue was severe. In the T2DM-MI + sh-ANRIL group, cardiomyocyte staining was basically uniform, the appearance was basically normal, and slight hypertrophy with a small amount of myocardial necrosis and mild inflammatory infiltration were found in the infarct area. In addition, the blue-stained collagen fibres were more severe in the T2DM-MI and T2DM-MI + vector groups than in the control group. In addition, ANRIL overexpression aggravated collagen fibres and ANRIL knockdown alleviated collagen fibres compared with the collagen fibres in the T2DM-MI + vector group.

3.5. Effects of lncRNA ANRIL on myocardial cell apoptosis in the T2DM-MI mice

TUNEL staining was used to detect the effects of ANRIL on myocardial cell apoptosis in the T2DM-MI mice. As shown in Fig. 5, the percentage of apoptotic myocardial cells in the T2DM-MI group was significantly increased compared with that in the control group ($p < 0.001$). We also found that ANRIL overexpression significantly increased the apoptotic index compared with that in the T2DM-MI + vector group ($p < 0.01$), and ANRIL knockdown exerted the opposite effect ($p < 0.01$).

3.6. Effects of lncRNA ANRIL on the expression of myocardial fibrosis-related proteins in the T2DM-MI mice

TGF-β1 was reported to induce the proliferation of cardiac fibroblasts and promote the generation of extracellular matrix.[25] In addition, fibrillar collagen types I and III are the major components of the myocardial collagen matrix.[26]

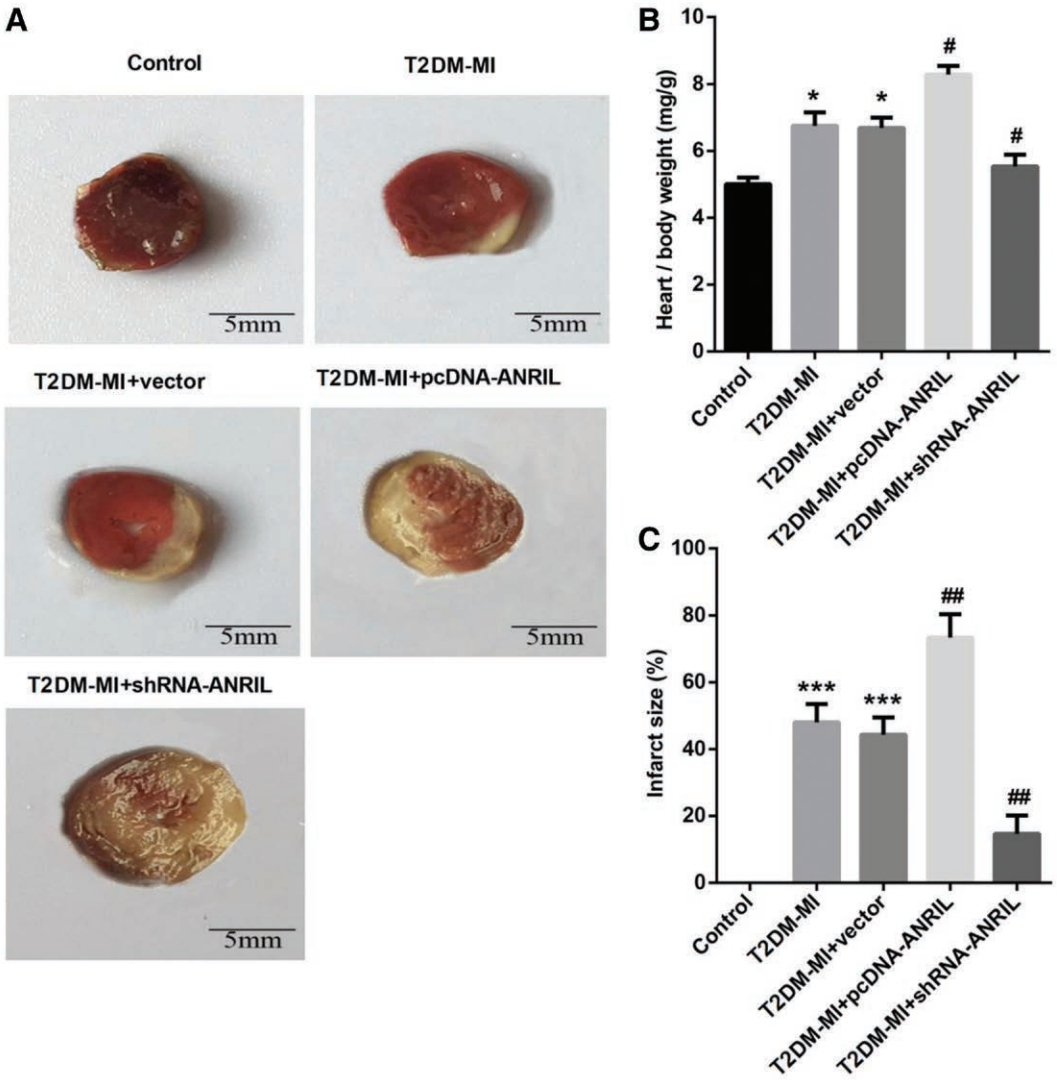

Fig. 3 Effects of lncRNA ANRIL on cardiac function and pathological changes in the T2DM-MI mice. (A) Comparison of the ischaemic infarct area between groups by TTC staining. Normal tissues are red, and ischaemic infarct areas are pale white. Compared with the T2DM + vector group, the ANRIL overexpression group had an increased infarct area, and the ANRIL knockdown group had a decreased infarct area. (B) ANRIL overexpression significantly increased the heart/body weight ratio compared to that in the T2DM + vector group. ANRIL knockdown exerted the opposite effect. (C) The infarct size in the T2DM-MI mice was significantly increased compared with that in the control group. ANRIL knockdown exerted the opposite effect. n = 10 in each group. $^{*}p < 0.05$ and $^{***}p < 0.001$ *vs.* control group, $^{\#}p < 0.05$ and $^{\#\#}p < 0.01$ *vs.* T2DM + vector group.

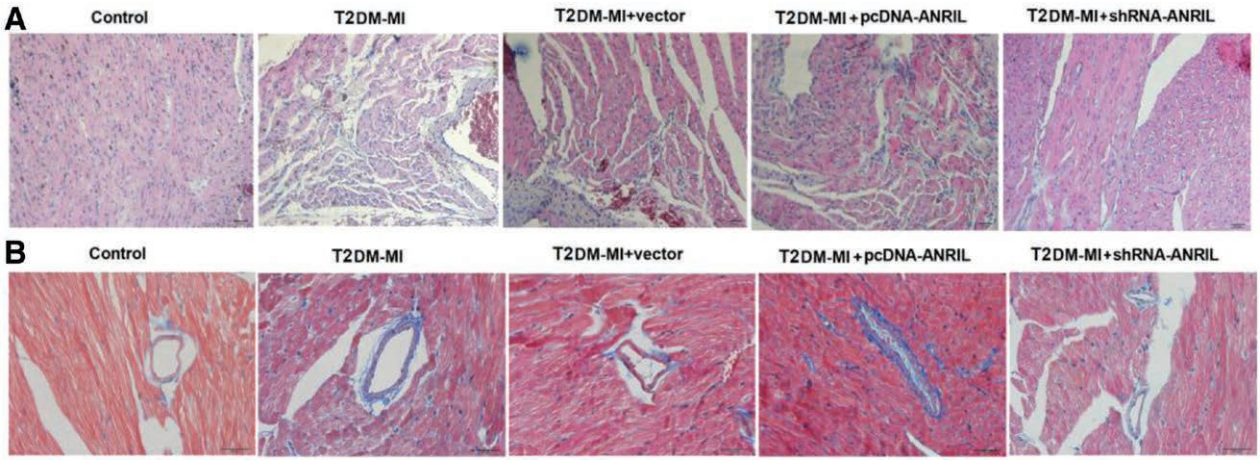

Fig. 4 Effects of lncRNA ANRIL on myocardial pathology and fibrosis in T2DM-MI mice. (A) HE staining was performed to determine myocardial pathology in the groups. (B) Masson's trichrome staining was performed to delineate the area of fibrosis in the myocardium of the groups. The fibrotic area was stained blue and viable area was stained red. n = 10 in each group. At 4 weeks after the surgery, hearts were sectioned from the apex to the base into five slices for staining. n = 10 in each group.

Here, the effects of ANRIL on the expression of the myocardial fibrosis-related proteins TGF-β1, collagen I and III in the T2DM-MI mice were analysed. As shown in Fig. 6, the protein expression of TGF-β1, collagen I and collagen III in the T2DM-MI group was significantly increased compared with that in the control group ($p < 0.01$, $p < 0.05$, and $p < 0.01$, respectively). We also found that ANRIL overexpression significantly increased the protein expression of TGF-β1, collagen I and III compared with that in the T2DM-MI + vector group ($p < 0.01$, $p < 0.05$, and $p < 0.05$, respectively). ANRIL knockdown exerted the opposite effects ($p < 0.05$, $p < 0.05$, and $p < 0.05$, respectively).

4. DISCUSSION

In this study, we first found that ANRIL was upregulated in peripheral venous blood from patients with T2DM-MI. In the established T2DM-MI mouse model, we also found that ANRIL was upregulated in myocardial tissues. Consistent with our results, ANRIL expression was increased in the mice with T2DM and cerebral infarction.[27] Broadbent et al.[16] indicated that the susceptibility to coronary artery disease and diabetes is encoded by distinct, tightly linked single-nucleotide polymorphisms (SNPs) in the ANRIL locus on Chr9p. ANRIL is essential in mediating Chr9p21 associations and has been reported to play an important role in many

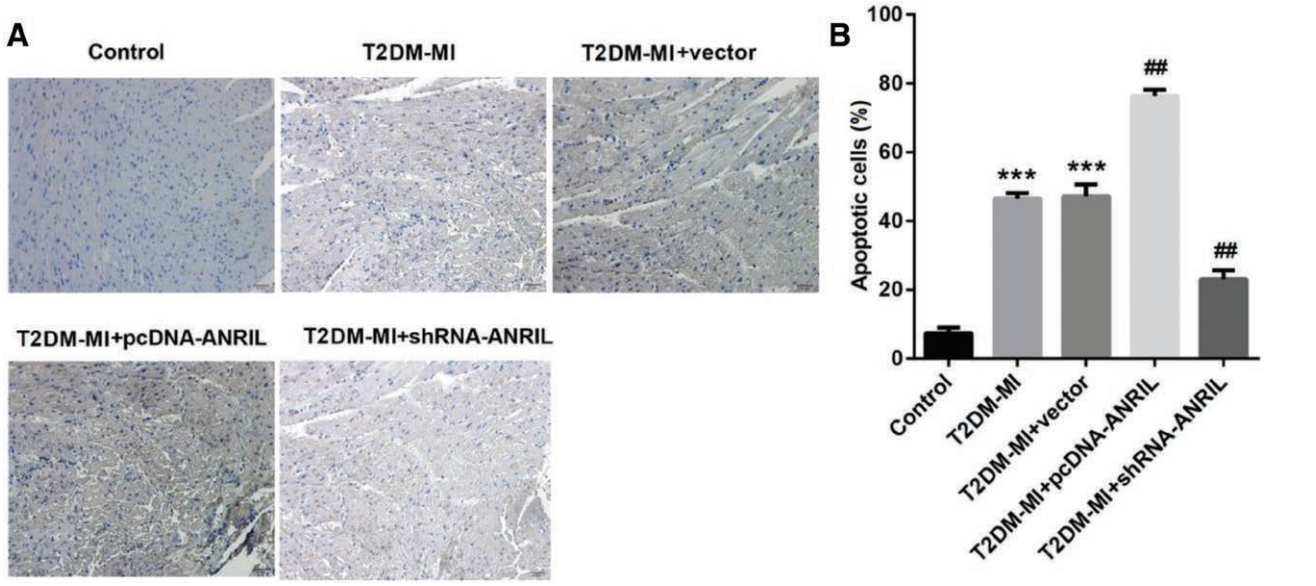

Fig. 5 Effects of lncRNA ANRIL on myocardial cell apoptosis in the T2DM-MI mice. TUNEL staining was used to detect the effects of ANRIL on myocardial cell apoptosis in T2DM-MI mice. ANRIL overexpression significantly increased the apoptotic index compared with that in the T2DM-MI + vector group, and ANRIL knockdown exerted the opposite effect. n = 10 in each group. At 4 weeks after the surgery, hearts were sectioned from the apex to the base into five slices for staining. n = 10 in each group. $^{***}p < 0.001$ *vs.* control group and $^{\#\#}p < 0.01$ *vs.* T2DM + vector group.

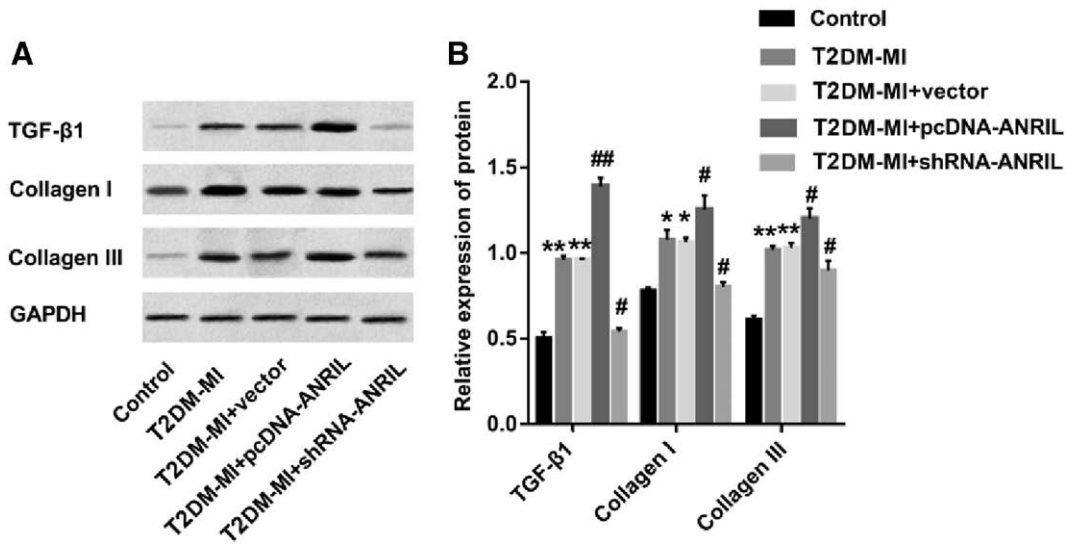

Fig. 6 Effects of lncRNA ANRIL on the expression of myocardial fibrosis-related proteins in the T2DM-MI mice. ANRIL overexpression significantly increased the protein expression of TGF-β1, collagen I and III in myocardial tissues compared with that in the T2DM-MI + vector group, and ANRIL knockdown exerted the opposite effect. n = 10 in each group. $^{*}p < 0.05$, $^{**}p < 0.01$ *vs.* control group, $^{\#}p < 0.05$ and $^{\#\#}p < 0.01$ *vs.* T2DM + vector group.

diseases, including T2DM.[13] A meta-analysis also provided accurate and comprehensive estimates of the association of some genetic variants at Chr9p21 with T2DM.[28] In addition, variants in ANRIL were found to contribute to MI risk in a Chinese Han population.[15]

We then analysed the effect of ANRIL on cardiac function and pathological changes in the T2DM-MI mice. The results indicated that ANRIL overexpression caused cardiac dysfunction and increased the heart/body weight rate and infarct size in the T2DM-MI mice. In contrast, ANRIL knockdown exerted the opposite effects. Pfeffer et al.[29] indicated that rats with infarctions greater than 46% had congestive heart failure, with reduced cardiac output, elevated filling pressures, and a minimal capacity to respond to pre- and after-load stresses. The heart/body weight coefficient has been used to characterize myocardial hypertrophy and could be used to assess myocardial hypotrophy.[22] Thus, our results suggested that ANRIL contributed to heart failure and myocardial hypotrophy in the T2DM-MI mice.

Adult cardiac myocytes are terminally differentiated cells that have lost their ability to divide. A large number of studies found that apoptosis in cardiac myocytes is involved in the transition from cardiac compensation to decompensated heart failure.[30] Myocardial fibrosis provides a structural basis for the appearance of diastolic dysfunction. In addition, it is the quality rather than the quantity of tissue that accounts for pathological left ventricular hypertrophy with associated adverse cardiovascular events and sudden cardiac death.[31] Fibrillar collagen types I and III are the major components of the myocardial collagen matrix.[26] It has been found that collagen type I represents nearly 80% of the total collagen protein, while collagen III is present in lower proportions (approximately 11%).[26] The fibrillar collagens serve as tethers between muscle cells, muscle fibres, and blood vessels and provide a scaffolding that supports the muscular and vascular compartments.[32] In this study, in ANRIL-overexpressed T2DM-MI mice, myocardial fibres in a disordered arrangement, and a large number of fibroblasts in the myocardial vasculature and mesenchyme and severe hyperplasia of fibrous connective tissue were also observed. Furthermore, ANRIL overexpression significantly increased the apoptotic index in the T2DM-MI mice. Moreover, overexpression of ANRIL caused myocardial cell apoptosis and increased the expression of the myocardial fibrosis-related proteins TGF-β1, collagen I and III in the T2DM-MI mice. Based on these findings, it seems that ANRIL overexpression leads to myocardial fibre cell apoptosis and myocardial fibrosis by enhancing the components of the myocardial collagen matrix in T2DM-MI mice.

In conclusion, our study indicated that ANRIL was upregulated in peripheral venous blood from patients with T2DM-MI and in myocardial tissue from the established T2DM-MI mice. ANRIL overexpression caused cardiac dysfunction and led to heart failure, myocardial hypotrophy, myocardial fibre cell apoptosis, and myocardial fibres in the T2DM-MI mice. Our findings demonstrated that ANRIL may be involved in the progress and development of T2DM-MI, which might provide novel ideas for the prevention and treatment of cardiovascular diseases.

REFERENCES

1. Woods KL, Samanta A, Burden AC. Diabetes mellitus as a risk factor for acute myocardial infarction in Asians and Europeans. *Br Heart J* 1989;**62**:118–22.
2. Vegad DAM, Varu DMS, Rathod DMM, Jani HA, Savalia DCVA. Study of first episode of acute myocardial infarction in type 2 diabetes mellitus patients. *Am J Cardiol* 2012;**112**:73–8.
3. Ling L, Shen Y, Wang K, Jiang C, Fang C, Ferro A, et al. Worse clinical outcomes in acute myocardial infarction patients with type 2 diabetes mellitus: relevance to impaired endothelial progenitor cells mobilization. *PLoS One* 2012;**7**:e50739.
4. Pickup JC. Inflammation and activated innate immunity in the pathogenesis of type 2 diabetes. *Diabetes Care* 2004;**27**:813–23.
5. Tay Y, Rinn J, Pandolfi PP. The multilayered complexity of ceRNA crosstalk and competition. *Nature* 2014;**505**:344–52.
6. Geisler S, Coller J. RNA in unexpected places: long non-coding RNA functions in diverse cellular contexts. *Nat Rev Mol Cell Biol* 2013;**14**:699–712.
7. Ulitsky I, David Bartel P. lincRNAs: genomics, evolution, and mechanisms. *Cell* 2013;**154**:26–46.
8. Oliaei NA, Shahryari A, Majidzadeh K. Long noncodin RNA ANRIL and it's intronic gene, P15 INK4B, revealed different expression patterns in breast cancer 2013 Tabriz University of Medical Sciences.
9. Xu X, Wan X, Zhang Z. Long non-coding RNA ANRIL promotes tumorigenesis in glioma via MAPK signaling pathways. *Int J Clin Exp Pathol* 2016;**9**:10803–9.
10. Nie FQ, Sun M, Yang JS, Xie M, Xu TP, Xia R, et al. Long noncoding RNA ANRIL promotes non small cell lung cancer cells proliferation and inhibits apoptosis by silencing KLF2 and P21 expression. *Mol Cancer Ther* 2015;**14**:268–77.
11. Zhang EB, Kong R, Yin DD, You LH, Sun M, Han L, et al. Long noncoding RNA ANRIL indicates a poor prognosis of gastric cancer and promotes tumor growth by epigenetically silencing of miR-99a/miR-449a. *Oncotarget* 2014;**5**:2276–92.
12. Patel RS, Su S, Neeland IJ, Ahuja A, Veledar E, Zhao J, et al. The chromosome 9p21 risk locus is associated with angiographic severity and progression of coronary artery disease. *Eur Heart J* 2010;**31**:3017–23.
13. Congrains A, Kamide K, Ohishi M, Rakugi H. ANRIL: molecular mechanisms and implications in human health. *Int J Mol Sci* 2013;**14**:1278–92.
14. Holdt LM, Beutner F, Scholz M, Gielen S, Gäbel G, Bergert H, et al. ANRIL expression is associated with atherosclerosis risk at chromosome 9p21. *Arterioscler Thromb Vasc Biol* 2010;**30**:620–7.
15. Cheng J, Cai MY, Chen YN, Li ZC, Tang SS, Yang XL, et al. Variants in ANRIL gene correlated with its expression contribute to myocardial infarction risk. *Oncotarget* 2017;**8**:12607–19.
16. Broadbent HM, Peden JF, Lorkowski S, Goel A, Ongen H, Green F, et al. Susceptibility to coronary artery disease and diabetes is encoded by distinct, tightly linked SNPs in the ANRIL locus on chromosome 9p. *Hum Mol Genet* 2008;**17**:806–14.
17. Sampaio CR, Franco DR, Goldberg DJ, Baptista J, Eliaschewitz FG. Glucose control in acute myocardial infarction: a pilot randomized study controlled by continuous glucose monitoring system comparing the use of insulin glargine with standard of care. *Diabetes Technol Therapeut* 2012;**14**:117–24.
18. Wang X, Zhao X, Dorje T, Yan H, Qian J, Ge J. Glycemic variability predicts cardiovascular complications in acute myocardial infarction patients with type 2 diabetes mellitus. *Int J Cardiol* 2014;**172**:498–500.
19. Kamalakkannan N, Stanely MPP. Rutin improves the antioxidant status in streptozotocin-induced diabetic rat tissues. *Mol Cell Biochem* 2006;**293**:211–9.
20. Arulmozhi DK, Hanker AVLB. Neonatal streptozotocin-induced rat model of Type 2 diabetes mellitus: a glance. *Indian J Pharmacol* 2004;**36**:217–21.
21. Rodrigues ACT, Hataishi R, Ichinose F, Bloch KD, Derumeaux G, Picard MH, et al. Iconography : relationship of systolic dysfunction to area at risk and infarction size after ischemia-reperfusion in mice. *Monum Nippon* 2007;**62**:323–45.
22. Cunha DF, Cunha SF, Reis MA, Teixeira VP. Heart weight and heart weight/body weight coefficient in malnourished adults. *Arq Bras Cardiol* 2002;**78**:382–87.
23. Wu A, Zhai J, Zhang D, Lou L, Zhu H, Gao Y, et al. Effect of Wenxin Granule on ventricular remodeling and myocardial apoptosis in rats with myocardial infarction. *Evid Based Complement Alternat Med* 2013;**2013**:967986.
24. Livak KJ, Schmittgen TD. Analysis of relative gene expression data using real-time quantitative PCR and the 2(-Delta Delta C(T)) Method. *Methods* 2001;**25**:402–8.
25. Liu JC, Wang F, Xie ML, Cheng ZQ, Qin Q, Chen L, et al. Osthole inhibits the expressions of collagen I and III through Smad signaling pathway after treatment with TGF-β1 in mouse cardiac fibroblasts. *Int J Cardiol* 2017;**228**:388–93.
26. Souza RRD. Aging of myocardial collagen. *Biogerontology* 2002;**3**:325–35.
27. Bo Z, Dan W, Ji TF, Lei S, Yu JL. Overexpression of lncRNA ANRIL up-regulates VEGF expression and promotes angiogenesis of diabetes mellitus combined with cerebral infarction by activating NF-κB signaling pathway in a rat model. *Oncotarget* 2017;**8**:17347–59.

28. Cugino D, Gianfagna F, Santimone I, De GG, Donati MB, Iacoviello L, et al. Type 2 diabetes and polymorphisms on chromosome 9p21: a meta-analysis. *Nutr Metabol Cardiovasc Dis* 2012;**22**: 619–25.
29. Pfeffer MA, Pfeffer JM, Fishbein MC, Fletcher PJ, Spadaro J, Kloner RA, et al. Myocardial infarct size and ventricular function in rats. *Circ Res* 1979;**44**:503–12.
30. Hasegawa K, Iwai-Kanai E, Sasayama S. Neurohormonal regulation of myocardial cell apoptosis during the development of heart failure. *J Cell Physiol* 2001;**186**:11–18.
31. Weber KT, Brilla CG, Janicki JS. Myocardial fibrosis: functional significance and regulatory factors. *Cardiovasc Res* 1993;**27**:341–8.
32. Fibrosis POM. Patterns of myocardial fibrosis. *J Mol Cell Cardiol* 1989;**21**:121–31.